Università di Pisa
Physics Department

PhD PreThesis

Out-of-equilibrium dynamics in round-trip and dissipation protocols

Behavior of the quantum phase transitions

Author:
Francesco Tarantelli

Supervisor:
Prof. Ettore Vicari

Session 2023/2024

Contents

Introduction

The progress achieved in the control of nano-scales many-body systems has recently renewed the interest in understanding the out-of-equilibrium dynamic in quantum spin models [1, 2]. Out-of-equilibrium, these efforts provided, for instance, a characterization of the unusual spreading of correlations and entanglement [3, 4, 5, 6, 7, 8, 9, 10], as well as of the thermalization [11, 12, 13, 14], in condensed-matter analogs of confined systems.

A deeper comprehension of the time evolution of the critical correlations and entanglement spreading is indeed sought by both the theoretical and experimental communities [15].

In the realm of many-body systems, intriguing out-of-equilibrium phenomena come to the forefront as these systems undergo phase transitions. Even when the timescale (ts) for varying system parameters is significantly extended, large-scale critical modes fail to reach equilibrium. This leads to a rich tapestry of dynamic phenomena at phase transitions, including hysteresis, coarsening, Kibble-Zurek (KZ) defect production [16, 17, 18, 19], aging, and more. Such phenomena have been explored extensively in both theoretical and experimental settings, spanning classical and quantum phase transitions (see, for instance, Refs. [20, 21, 22, 23, 24, 1, 25] and related references).

Out-of-equilibrium scaling behaviors tend to emerge when slowly traversing a critical point, especially when doing so in the large-timescale (ts) limit. These scaling behaviors depend on several factors, including the nature of the transition (classical or quantum), its universality class, and the specific characteristics of critical dynamics in classical systems (as detailed in Refs. [17, 19, 24, 1].). Slow, or quasiadiabatic, passages through these critical points enable researchers to unveil universal features related to the emergence of long-range modes during thermal and quantum critical phenomena.

In both classical and quantum contexts, many-body systems are described by Hamiltonians that can be expressed as:

$$H(t) \equiv H[w(t)] = H_c + w(t)H_p \ , \tag{1}$$

Here, $w(t)$ represents a time-dependent Hamiltonian parameter, while H_c and H_p are time-independent components. H_c serves as the critical Hamiltonian at the transition point, which might denote a quantum continuous transition driven by quantum fluctuations or a classical continuous transition fueled by thermal fluctuations. H_p, on the other hand, embodies a nontrivial, relevant perturbation. Within quantum many-body models, it's generally assumed that $[H_c, H_p] \neq 0$. The tunable parameter w controls the strength of the coupling with the perturbation H_p, and it's considered a relevant parameter guiding the continuous transition.

Consequently, $w_c = 0$ marks the transition point. To explore the scaling properties of out-of-equilibrium dynamics during phase transitions, researchers employ time-dependent protocols where parameters like $w(t)$ are slowly varied, linearly in time, across the transition point at $w_c = 0$, employing a large timescale t_s.

The inevitable growth of out-of-equilibrium dynamics during phase transitions in the thermodynamic limit arises because large-scale modes cannot equilibrate the long-range critical correlations that emerge at the transition point. This holds true even when the parameter w changes very slowly, and even in the limit of large timescales. Consequently, when starting from equilibrium states at the initial value w_i, the system cannot pass through equilibrium states corresponding to the values of $w(t)$ across the transition point. This departure from equilibrium results in distinctive out-of-equilibrium dynamic scaling phenomena, especially when observed in the limit of large timescale ts. This scenario gives rise to the Kibble-Zurek (KZ) problem, which concerns the scaling behavior of the final number of defects after slow passages through continuous transitions from the disordered phase to the ordered phase.

Out-of-equilibrium scaling behaviors in many-body systems undergoing slow transitions across classical and quantum critical points exhibit intriguing similarities. These phenomena can be comprehensively analyzed within unified renormalization-group (RG) frameworks, analogous to those employed to understand equilibrium scaling behaviors, which can be related through quantum-to-classical mappings. However, it's important to note that the out-of-equilibrium scaling behavior in classical systems depends on the chosen dynamics, whether it involves purely relaxational processes or conserved quantities, leading to different dynamic features.

The first part embarks on an investigation into the effects of slow round-trip variations in the Hamiltonian parameter $w(t)$, which entail multiple crossings of quantum and thermal transitions. These round-trip protocols are initiated from equilibrium conditions, traverse the transition point, and return to their initial state, with the timescale ts governing the slow-crossing regime in the large-t_s limit.

The exploration encompasses both classical and quantum continuous transitions, characterized by emerging long-range correlations. Unified RG frameworks are utilized to derive general dynamic scaling behaviors applicable to both classical and quantum transitions, considering large timescale ts for round-trip KZ protocols and large system sizes L. This study builds upon existing dynamic RG frameworks used in standard one-way KZ protocols.

Notably, this study focuses on transitions between gapped phases characterized by short-range correlations, avoiding the complexities associated with gapless modes in ordered phases. This approach differs from standard KZ protocols, where systems transition from a disordered phase to ordered phases characterized by long-range correlations, leading to additional dynamic effects at large timescales, such as coarsening phenomena or the emergence of massless Goldstone excitations.

As the ensuing discussions reveal, while there are analogies in the scaling behaviors observed in standard one-way KZ protocols at classical and quantum transitions, these similarities only partially extend to round-trip KZ protocols. Significant differences emerge, especially when the extreme value $w_f > 0$ is held fixed and finite at the return point, a situation where classical systems exhibit well-defined scaling phenomena with hysteresis-like scenarios. In contrast, quantum systems encounter challenges in observing scaling behaviors along the return path due to rapidly oscillating relative phases between relevant quantum states, making the

return trajectory highly sensitive to protocol parameters, such as w_f and system size. This sensitivity is a consequence of the quantum unitary nature of dynamics, and it bears similarities to the behavior observed in quantum two-level models subject to round-trip protocols, akin to the Landau-Zener-Stückelberg problem.

Since any experimental device is unintentionally coupled to the environment, a particular emphasis is put on the dynamics of *open quantum systems* [26].

When the interactions of a quantum system with its surroundings are sufficiently weak, the real-time evolution of such apparatuses emerges from the interplay between the unitary and dissipative dynamics of the whole setup [27]. These hypotheses are usually satisfied within *Lindblad* frameworks, which underpin the modelization of most atomic, molecular, and optical devices (AMO) [28]. In such cases, the system is described in terms of a density matrix ρ, and the time evolution is controlled by *Linblad Master equations*

$$\frac{d\rho}{dt} = \mathcal{L}[\rho]\,. \tag{2}$$

The system generally thermalizes to a Non-Equilibrium Steady-State (NESS) solution after a transitory time frame. However, determining whether the NESS is unique is a more subtle issue [29, 30]. A quantity of particular interest is the *Liouvillian gap*, hereafter denoted as Δ_λ. This energy scale sets the typical relaxation time required to make the NESS stand out, entailing a complete loss of information on the initial quantum state. Quantum memory devices, for example, would benefit from long relaxation times, therefore small Δ_λ [31].

Several works have addressed the nature of the Liouvillian gap in one-dimensional open quantum systems, considering different lattice geometries and dissipation sources also in integrable models [32]. Distinguished behaviors emerge when the dissipators are either isolated or in a relatively large number compared to the system size L. On the one hand, with bulk dissipation acting on the whole network, the system is gapped in several paradigmatic spin chains, such as XX, XXZ, and Ising models [33, 32, 34]. On the other hand, when the number of dissipative sources is constant, the Liouvillian gap generally vanishes with a distinctive power-law behavior in the thermodynamic limit, typically as $\sim L^{-3}$ [35, 36, 37]. The physical mechanisms tying together these two regimes are still unclear and are the main focus of the second part of this work [38].

In particular, we consider a lattice model tailored to unveil the crossover regime between the dissipation schemes presented. We investigate a $(1+1)$-dimensional Kitaev ring with local particle-decay dissipators arranged in a *sunburst* geometry [39, 40, 41]. Starting the protocol in the proximity of a Continuous Quantum Transition (CQT), we study the out-of-equilibrium dynamic using Renormalization Group (RG) arguments and Finite-Size Scaling (FSS) frameworks [42, 27].

Outline

In the **Chapter** 1, we introduce all the equations and the definitions useful to present the original results in the last two chapters. Indeed, we give a brief intro on the quantum phase transitions and, then, we explain two different mechanisms which send the system out-of-equilibrium regime: the Kibble-Zurek mechanism

and the Lindblad mechanism.

In the **Chapter** 2, we address the effect of a round-trip Kibble-Zurek protocol near a continuous quantum phase transitions, using the Finite Size Scaling framework. We will find results which diverge from the classic hysteresis cycle scenario.

In the **Chapter** 3, we analyze the effects of a local and a uniform dissipation process on a second-order transition. We will focus on the interplay between these two type of dissipation mechanism, trying to extract common properties and different behaviors.

Chapter 1

Out-of-equilibrium dynamics

1.1 Introduction

This chapter is devoted to introduce the basis and the notation associated with the analysis of quantum system in the presence of processes which generate the out-of-equilibrium dynamics. In particular, we start from system close their equilibrium quantum transition point and, then, we turn on two different time perturbations:

- an unitary round-trip process whose time-evolution is associated with an hermitian Hamiltonian;
- a dissipation process in which we put our quantum system in contact with external baths.

1.2 Equilibrium Quantum Transitions

1.2.1 Continuous Quantum Transition (CQT)

In the thermodynamic limit, i.e. infinite volume limit, same specific models could undergo a continuous phase transition. With the word phase, we intend the physical properties of the ground stare associated with the Hamiltonian and characterized by the values of the Hamiltonian parameters. If this phase changes driving one of this parameter, we are in the presence of a quantum transition and the point, in which that happens, is called transition point.

In the particular case of the CQT, the quantum ground-state properties are continuous close to the transition point, called also critical point. In this special point, the system develops a long-distance correlations and its microscopic behavior becomes negligible.

Independent from the local details, the global properties determine a notable universal critical behavior in which we collect different physical systems in universality class. In terms of the Renormalization Group (RG) theory, the critical point and its universal behavior ase associated the fixed points of the RG flux. Hence, if we call b the characteristic unit length of the system and if we define the RG transformation as the parameter rescaling respect b, the physical observables satisfy general scaling law unchanged along all the RG flux [43, 42].

From a physics point of view, we can interpret the factor b like the spatial correlation length ξ which diverges approching the critical point. According to

the renormalization group (RG) theory of critical phenomena, these global properties may be the spatial dimension- ality, the nature of the order parameter, the symmetry and the symmetry-breaking pattern [44].

Moreover, at CQTs the systems develop an equilibrium and dynamic scaling be- havior in the thermodynamic limit and their quantum functions satisfy scaling power laws characterized by universal critical exponents [45].

1.2.2 First Order Quantum Transition (FOQT)

Quasi-degenerate vacua naturally arise in the context of quantum phase transitions, after a spontaneous symmetry breaking. Their behavior and coexistence in the non-critical regime is governed by a first-order quantum transition.

It is characterized by the crossings of the lowest-energy states in the infinite-volume limit and in the absence of conservation laws [46]. Instead, in a finite system, the energy gap among these states remain different from zero, giving rise to the phenomenon of avoided level crossing.

FOQTs are associated with many important out-of-equilibrium effects s, including nucleations and metastability [20, 22], coarsening [47], and anomalous dependence on the boundary conditions [48, 49, 50, 51, 52].

1.2.3 Models

Quantum Ising

As a first toy model for the study of quantum phase transitions, we consider the quantum 1D Ising Model whose Hamiltonian is given by:

$$H(g,h) = -\sum_{x=1}^{L-1} \sigma_x^{(1)}\sigma_{x+1}^{(1)} - h\sum_{x=1}^{L} \sigma_x^{(1)} - g\sum_{x=1}^{L} \sigma_x^{(3)} \ ; \tag{1.1}$$

where L is the system size and $\sigma_x^{(k)}$ are the Pauli matrices on the x^{th} site.

This system develops a quantum critical behavior at $g = g_c = 1$ and $h = 0$, belonging to the 2D Classical Ising universality class [43]. Instead, when h is different from zero, the lowest states energy gap is not vanish.

Along the RG flux, the relevant parameters associated with the RG perturbations at the fixed point are $r = g - g_c$ and h. Their RG dimensions are respectively $y_r = 1/\nu = 1$ and $y_h = 15/8$, so that the length scale ξ of the critical modes behaves as $\xi \sim |g - g_c|^{-1/y_r}$ for $h = 0$, and $\xi \sim |h|^{-1/y_h}$ for $g = g_c$. The dynamic exponent z associated with the vanish critical gap $\Delta \sim \xi^{-z}$ at the transition point, is given by $z = 1$. The order parameter field, which distinguishes the two phases and is associated with the longitudinal operators $\sigma_x^{(1)}$, has a RG dimension equal to $y_l = d + z - y_h = 1/8$, while that associated with the transverse operator $\sigma_x^{(3)}$ is equal to $y_t = d + z - y_r = 1$.

In the ferromagnetic phase $g < 1$, the model undergoes a FOQT at $h = 0$. Across this point, the system remains non-critical and displays exponential decay of the correlation functions.

For $h = 0$, the model presents a level-crossing of the two lowest-energy state in the infinite volume limit, where the energy gap closes exponentially for $L \to \infty$, e.g. for open boundary condition [53]:

$$\Delta(g, L) = 2g^L(1 - g^2)\Big[1 + \mathcal{O}(g^{2L})\Big] \ . \tag{1.2}$$

In the limit of small longitudinal magnetic field, i.e. $|h \ll 1|$, the system presents a Zeeman-like gap in energy between the 2 lowest states which introduces another symmetry-breaking of the degeneracy. We can express an approximation of this gap using standard perturbation theory in h [54]:

$$\mathcal{E}(g, h \to 0, L) \simeq 2h \sum_{j=1}^{L} |\langle \sigma_j^{(3)} \rangle| \simeq 2hLM_0(g) \ , \tag{1.3}$$

with $M_0 = (1 - g^2)^{1/8}$ the approximated longitudinal magnetization in the constrains $h = 0$ and $L \to \infty$.

Kitaev chain

Now, we introduce the following lattice model, called Kitaev model [55], whose Hamiltonian describes the fermions interaction with the lattice and is given by:

$$\hat{H} = -\sum_{x=1}^{L-1} (\hat{c}_x^\dagger \hat{c}_{x+1} + \hat{c}_x^\dagger \hat{c}_{x+1}^\dagger + \text{h.c.}) - \mu \sum_{x=1}^{L} \hat{n}_x \ , \tag{1.4}$$

where $\hat{n}_x \equiv \hat{c}_x^\dagger \hat{c}_x$ is the number operator on the site x, and the operators $\hat{c}_x, \hat{c}_x^\dagger$ satisfy the canonical anticommutation relations, thus $\{\hat{c}_x, \hat{c}_y\} = \{\hat{c}_x^\dagger, \hat{c}_y^\dagger\} = 0$ and $\{\hat{c}_x, \hat{c}_y^\dagger\} = \delta_{xy}$. Applying the Jordan-Wigner transformation [43], the Kitaev ring can be exactly mapped into a quantum Ising chain with a transverse field [56]. We point out that the transformation does not preserve also the same boundary conditions, so attention should be paid when recasting Eq. (1.4) in its bosonic counterpart [27]. Nonetheless, many bulk properties of the Ising model, such as the critical exponents at the CQT point, are preserved by the mapping; in fact, these phase transition belongs to the same universality class of the 1D quantum Ising model.

The quantum Ising model with a transverse field is one of the most common theoretical laboratories where fundamental issues on quantum phase transition can be addressed, given our deep knowledge of the quantum correlations [43]. The model is characterized by a $\mathbb{Z}_2$ global symmetry under spin reflection along the longitudinal axis. In Eq. (1.4), this symmetry is implemented by the transformation that maps $\hat{c}_x^{(\dagger)} \to -\hat{c}_x^{(\dagger)}$. At zero temperature, the ground state experiences a CQT at $\mu_c = -2$ and the $\mathbb{Z}_2$ symmetry is then spontaneously broken. The critical point separates a paramagnetic phase ($|\mu| < |\mu_c|$), where correlation functions are exponentially dumped, from an ordered phase ($|\mu| < |\mu_c|$), where correlation functions are instead long-range ordered. Close to the critical point, the correlation length diverges as $\xi \sim |\mu - \mu_c|^{-\nu}$, where $\nu = 1/y_g = 1$ for Ising transitions. The gap Δ, which describes the energy difference between the first excited state and the ground state, vanishes instead as $\Delta \sim \xi^{-z}$ with $z = 1$.

1.3 Unitary time-evolution

1.3.1 Quench

In the quench protocol, we define a family of Hamiltonians of type:

$$H(\bar{\mu}) = H_o + \bar{\mu} P \ , \tag{1.5}$$

where in this case the scaling variable $\bar{\mu}$ tunes the strength of the perturbation P such that $\Big[H_o, P\Big] \neq 0$ and H_o is the unperturbed Hamiltonian whose parameters assume their critical values.

In this quench protocol, at $t = t_0$ the system starts in the ground state of the Hamiltonian associated with an initial value $\bar{\mu}_i$. Then, at time $t > 0$, we suddenly change the coupling from $\bar{\mu}$ to $\bar{\mu}_i$ and we follow the corresponding evolution of the system.

To express a possible scaling law, we define a further scaling variable associated with the time:

$$\theta = t\Delta \ , \tag{1.6}$$

which is obtained by recalling that the inverse energy difference of the lowest states is proportional to the relevant time scale of the critical modes.

1.3.2 Kibble-Zurek mechanism

The Kibble-Zurek(KZ) mechanism is related to the amount of final defects after slow passages through continuous transition, from disordered to the ordered phase [16, 17, 18, 19, 57]. This type of out-of-equilibrium process is several studied both analytically-numericallly [24, 1, 47, 58] both experimentally [23, 25].

The large-scale modes, associated with the changes of the transition tuning parameter, are insufficient to equilibrate the long-distance critical correlations. Even in the large time variation regime, the out-of-equilibrium dynamics grows in the thermodynamic limit. In other words, when the system evolves, starting from an equilibrium state, the time-evolution is different from an adiabatic dynamics and the system does not pass through equilibrium states.

In this scenario, the out-of-equilibrium regime is always describable in terms of the RG framework and the equilibrium scaling behaviors can be related by the quantum to classical mapping [58, 43].

1.4 Time-evolution in Open Quantum Systems

1.4.1 Lindblad framework

To model the weak interaction between the previous quantum model and the surrounding environment, we consider local external baths each in contact with only site of the system chain. We work under the Born-Markov and secular approximations, so dissipators can be effectively modeled employing Lindblad quantum jump operators $\hat{L}_x$. In this limit, the time evolution of the density matrix can be described by Markovian master equations in the Lindblad form as [26, 36, 59]:

$$\frac{d\rho}{dt} = \mathcal{L}[\rho] = -i\Big[H, \rho\Big] + \mathbb{D}[\rho] \ ; \tag{1.7}$$

where $\mathcal{L}$ is the Liouville superoperator, and $\mathbb{D}$ is the corresponding dissipation term, whose strength is regulated by the coupling w:

$$\mathbb{D}[\rho] = w \sum_{x \in \mathcal{I}} \mathbb{D}_x[\rho] \ , \tag{1.8}$$

$$\mathbb{D}_x[\rho] = \hat{L}_x \rho \hat{L}_x^\dagger - \frac{1}{2}\Big\{\rho, \hat{L}_x^\dagger \hat{L}_x\Big\} \ ; \tag{1.9}$$

where we indicate with $\mathcal{I}$ the set of the external baths in contact with the quantum system.

1.4.2 Liouvillian gap

Let us consider the following equation:

$$\widetilde{\mathcal{L}}[\widetilde{\rho}_i] = \lambda_i \widetilde{\rho}_i \ , \qquad \lambda_i \in \mathbb{C} \ ; \tag{1.10}$$

where $\widetilde{\mathcal{L}}$ is the (non-hermitian) Lindblad superoperator after the Choi-Jamiolkowski isomorphism [26, 60], and $\widetilde{\rho}_i$ is the density matrix eigen-operator associated with the complex eigenvalue λ_i. In a few words, the transformation we have mentioned sends the density matrix ρ to $\widetilde{\rho}$ through the mapping:

$$\rho_{ij} \left|i\right\rangle \left\langle j\right| \longrightarrow \widetilde{\rho}_{ij} \left|i\right\rangle \left|j\right\rangle \ . \tag{1.11}$$

Therefore, the vectorized $\widetilde{\rho}$ lives in a 4^L-dimensional Hilbert space. In this basis, the action of $\widetilde{\mathcal{L}}$ on $\widetilde{\rho}$ can be written as follows:

$$\widetilde{\mathcal{L}} = -i\big(\hat{H} \otimes \hat{\mathbb{I}} - \hat{\mathbb{I}} \otimes \hat{H}^t\big) + w \sum_{x \in \mathcal{I}} \hat{L}_x \otimes \hat{L}_x^* \tag{1.12}$$

$$- \frac{w}{2} \sum_{x \in \mathcal{I}} \big(\hat{L}_x^\dagger \hat{L}_x \otimes \hat{\mathbb{I}} + \hat{\mathbb{I}} \otimes \hat{L}_x^t \hat{L}_x^*\big) \ . \tag{1.13}$$

It can be shown that all eigenvalues of $\widetilde{\mathcal{L}}$ satisfy $\mathrm{Re}\lambda_i \leq 0$ [26]. The zero mode of the above operator represents the steady-state solution, namely, the NESS of the system. If $\hat{L}_x$ is not hermitian, the density matrix corresponding to the steady-state solution is not proportional to the identity matrix [35]. We focus on the Liouvillian gap Δ_λ, which is the non-vanishing eigenvalue of $\mathcal{L}$ with the smallest real part:

$$\Delta_\lambda = -\max_i \mathrm{Re}\lambda_i \ . \tag{1.14}$$

This quantity controls the typical relaxation time of the longest-living eigenmode differing from the NESS.

Chapter 2

Round Trip variation of Hamiltonian parameter

2.1 Protocol

In the following, we focus on the round-trip protocol between gapped phase in the Kitaev wire described by the Hamiltonian (1.4) with antiperiodic boundary condition ($\hat{c}_{L+1} = -\hat{c}_1$). To fix the notation, we will take:

$$w = \mu - \mu_c \ . \tag{2.1}$$

We investigate the critical dynamics of closed systems assuming quasi-adiabatic variation of the parameter w across the critical point $w_c = 0$, e.g. following the standard KZ procedure:

- One starts from the ground state of the many-body system at $w_i < 0$, given by $|\Psi(t = t_i)\rangle \equiv |\Psi_0(w_i)\rangle$.
- Then the out-equilibrium unitary dynamics, ruled by the Schrödinger equation
$$\frac{\mathrm{d}\ |\Psi(t)\rangle}{\mathrm{d}t} = -i\, \hat{H}[w(t)]\ |\Psi(t)\rangle \ , \tag{2.2}$$
arises from a linear dependence of the time-dependent parameter $w(t)$, such as
$$w(t) = t/t_s \, , \tag{2.3}$$
up to a final value $w_f > 0$. Therefore the KZ protocol starts at time $t_i = t_s\, w_i < 0$ and stops at $t_f = t_s\, w_f > 0$. The parameter t_s denotes the time scale of the slow variations of the Hamiltonian parameter w.
- Then, for $t > t_f$, we complete the cycle by descreasing w from w_f to the original value w_i with the same time scale t_s.

To reduce the number of the free parameter, we consider a symmetric round-trip protocol with:

$$w_\star = w_f = -w_i \ , \tag{2.4}$$
$$t_\star = t_f = -t_i \ . \tag{2.5}$$

The resulting out-of-equilibrium evolution of the system can be investigated by monitoring observables and correlations at fixed time. One may consider the evolution of the adiabaticity function:

$$A(t) = |\langle \Psi_0[h(t)]|\Psi(t)\rangle| \ , \tag{2.6}$$

where $|\Psi_0[w(t)]\rangle$ is the ground state of the Hamiltonian $\hat{H}[w(t)]$, i.e. at instantaneous values of $w(t)$, while $|\Psi(t)\rangle$ is the actual time-dependent state evolving according to the Schrödinger equation (2.2). The adiabaticity function measures the overlap of the time-dependent state with the corresponding ground state of the Hamiltonian at the same $w(t)$. Since the protocol starts from the ground state associated with $w_i = w(t_i)$, we trivially have $A(t_i) = 1$. If the quantum evolution is adiabatic, then $A(t) = 1$ at any time. In the general case arising from the above KZ protocol, $A(t)$ is expected to depart from the initial value due to the impossibility of the system to adiabatically follow the changes of the function $w(t)$ across its critical value $w = 0$.

Note however that this is strictly true in the infinite-volume limit. In system of finite size L, there is always a sufficiently large time scale t_s, so that the system can evolve adiabatically, essentially because finite-size systems are always gapped, although the gap Δ at the CQT gets suppressed as $\Delta \sim L^{-z}$. The interplay between the size L and the time scale t_s gives rise to nontrivial out-of-equilibrium scaling behaviors, which can be studied within finite-size scaling (FSS) frameworks [61, 58].

Another interessant quantities useful to monitor the out-of equilibrium dynamics are:

- the substract definition of the particle density:

$$\rho_s(t) = \langle \Psi(t)|c_x^\dagger c_x|\Psi(t)\rangle - \rho_c \ ; \tag{2.7}$$

  where ρ_c is its corrispondent value at the critical point in the infinite-volume limit.

- The fermionic correlation functions:

$$C(x,t) = \langle \Psi(t)|c_j^\dagger c_{j+x} + \text{h.c.}|\Psi(t)\rangle \ , \tag{2.8}$$

  with $i, j \in [1, L/2]$ considering the translation invariance due to ABC.

2.2 Dynamic Finite Size Scaling

Let us discuss the scaling whitin a dynamic RG framework. In the limit of slow variation of the driven parameter w, the dynamic scaling is dependent from the universality class while we cross the CQT point. In this situation, the critical divergent of the equilibrium relaxation time t_r is correlated with the scale time t_s of the variation of the driven parameter w. In particular, t_r behaves as:

$$t_r \sim \xi^z \sim |w|^{-z\nu} \ . \tag{2.9}$$

In this way, the interplay of the various dimensionful scales of the problem (such as the time t, the time scale t_s, the system size L and the energy gap

$\Delta \sim L^{-z}$) characterizes the flux of the RG transformations, leading to the scaling laws for observables constructed from a local operator $O(\boldsymbol{x})$. The dynamic FSS of its expectation value O_s and its two-point correlation function G_O are expected to obey homogeneous scaling laws [58]:

$$O_s^{(a/b)}(t, t_s, w_\star, L) \simeq b^{-y_o}\mathcal{O}(b^{-z}t, b^{y_w}w(t), b^{y_w}w_\star, b^{-1}L) \ , \tag{2.10}$$

$$G_O^{(a/b)}(\boldsymbol{x}, t, t_s, w_\star, L) \simeq b^{-2y_o}\mathcal{G}(b^{-1}\boldsymbol{x}, b^{-z}t, b^{y_w}w(t), b^{y_w}w_\star, b^{-1}L) \ ; \tag{2.11}$$

where b is an arbitrary lenght scale and the superscripts (a) and (b) indicate the outward and return trajectories.

By fixing $b = L$, we find the dynamic FSS of the KZ procedure. Then, the asympotic dynamic behavior is obtained by taking $t_s \to \infty$ and $L \to \infty$, while the following scaling are kept fixed:

$$K = w(t)L^{y_w} \ , \qquad \Upsilon = t_s/L^{\zeta} \ , \tag{2.12}$$

$$\Theta_\star = w_\star t_s^{1-\kappa} \ , \qquad \Theta = w(t)t_s^{1-\kappa} = t/t_s^{\kappa} \ , \tag{2.13}$$

(note that $K = \Upsilon^{\kappa-1}\Theta$) where:

$$\zeta = y_w + z \ , \quad \kappa = z/\zeta \ , \quad 1-\kappa = y_w/\zeta \ . \tag{2.14}$$

The previous scaling variable and the corresponding exponent derive from the application of the relations $b = L$ and $w(t) = t/t_s$ to the scaling laws Eqs.(2.10).

The corresponding dynamic scaling laws of the adiabaticity (2.6) and the correlation functions (2.8) are given by:

$$A^{(a/b)}(t, t_s, w_\star, L) \simeq \mathcal{A}^{(a/b)}(\Upsilon, \Theta, \Theta_\star) \ , \tag{2.15}$$

$$C^{(a,b)}(x, t, t_s, w_\star, L) \simeq L^{-2y_c}\mathcal{C}^{(a/b)}(x/L, \Upsilon, \Theta, \Theta_\star) \ ; \tag{2.16}$$

where y_c is the RG dimension associated with the operator $\hat{c}$ and equal to $1/2$ [43]. Note that the values of these observables after the full cycle are different from those at the beginning:

$$\mathcal{A}^{(b)}(\Upsilon, \Theta = -\Theta_\star, \Theta_\star) \neq \mathcal{A}^{(a)}(\Upsilon, \Theta = -\Theta_\star, \Theta_\star) \ , \tag{2.17}$$

they coincide only in the adiabatic limit, i.e. $\Upsilon \to \infty$, when the time-evolved system explores all the equilibrium state at the corresponding value of $\Theta(t)$.

In the above scaling behavior (2.15)-(2.16), the scaling parameter Θ plays a fundamental role. While in the classic hysteresis-like scenario the relaxational dynamic lead to a well-defined dynamic scaling when keeping $w_\star > 0$ [62] fixed, the quantum case is more problematic. The radid oscillations, due to the unitary dynamics, make the return somehow chaotic and extremely sensitive to the protocol parameters. This implies, also, a non-convergent value at the end of the round-trip protocol in the large-$\Theta_\star$ limit.

The dynamic scaling is realized only when keeping $\Theta_\star$ fixed, in fact the relative quantum phase behave consistently with the scaling laws.

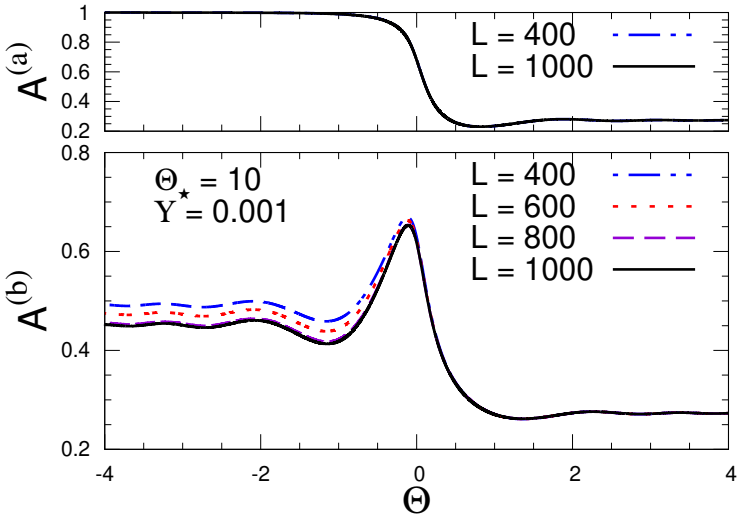

Figure 2.1: Round-trip dynamic FSS within the quantum Kitaev taev wire for a finite $\Theta_\star = 10$. We show results for the adiabaticity function $A(t, t_s, w_\star, L)$ at fixed $\Upsilon = t_s/L^\zeta = 0.001$ and $\Theta_\star = w_\star L^{1-\kappa} = 10$, for the outward (top) and return (bottom) branches of the round-trip KZ protocol, versus $\Theta = w(t)L^{1-\kappa}$, for various size L up to $L = 1000$. The values of the exponents y_w , ζ, and κ are reported in Eq.(2.18). The numerical results clearly support the dynamic scaling behavior given in Eq. (2.15).

2.3 Numerical Results

The numerical results are computed using a Kitaev wire with exact diagonalization techniques based on Nambu operators [63]. The resolution of the time-dependent Schrödinger equation is obtained through the 4^{th} order Runge-Kutta method.

This approach allows us to present simulation for lattice size L up to $L = 1000$. It is sufficient to achieve a robust evidence of the dynamic FSS outlined in the previous section. The corresponding critical exponents, associated with the quantum Kitaev model with driving chemical potential, are:

$$y_w = 1 \ , \qquad \zeta = 2 \ , \qquad \kappa = 1/2 \ . \tag{2.18}$$

We show numerical results for round-trip KZ protocols keeping $\Theta_\star$ finite, see Figs. 2.1 and 2.2, for the adiabaticity and the correlation functions. These plots support the dynamic FSS reported in the scaling laws in Eqs. (2.15)-(2.16).

2.3.1 The large-$\Theta_\star$ limit

We now discuss the large-$\Theta_\star$ limit which turns out to be quite problematic in quantum round-trip KZ protocols. To observe it, we focus on the end of the outward branch (a) and of the return branch (b) for KZ protocols with different $\Theta_\star$ (the "inversion-point"), to check their large-$\Theta_\star$ convergence, for some interval of values of $\Theta_\star$ and fixed L.

The observables at the end of the outward branch oscillate, with a frequency that becomes larger and larger with increasing $\Theta_\star$, as shown in Fig. 2.3 , and the

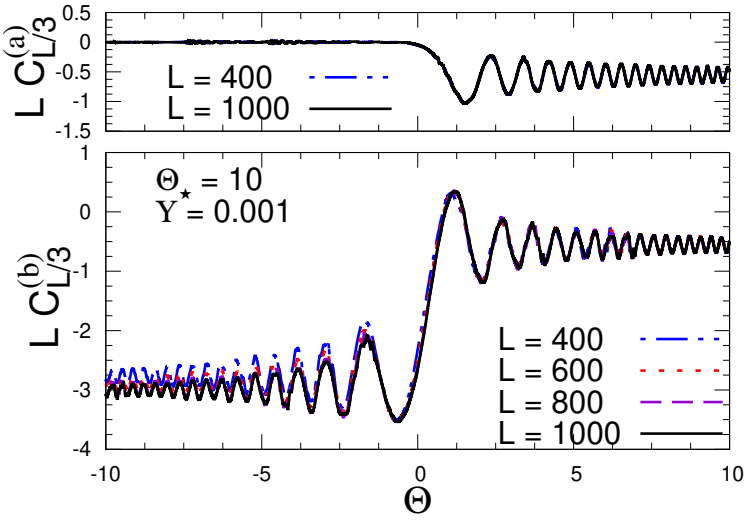

Figure 2.2: Round-trip dynamic FSS within the quantum Kitaev taev wire for a finite $\Theta_\star$. We show results for two-point function $C(x,t,t_s,w_\star,L)$ at fixed $X = x/L = 1/3$, $\Upsilon = t_s/L^\zeta = 0.001$ and $\Theta_\star = w_\star L^{1-\kappa} = 10$, for the outward (top) and return (bottom) branches of the round-trip KZ protocol, versus $\Theta = w(t)L^{1-\kappa}$, for various size L up to $L = 1000$. The numerical results clearly support the dynamic scaling behavior given in Eq. (2.16).

oscillations observed after the whole cycle are strongly correlated to those at the end of the first branch, doubling the frequency.

The above results strongly suggest that in quantum many-body systems the large-$\Theta_\star$ limit of the dynamic KZ scaling does not exist along the return trajectories, and, as a consequence, no dynamic scaling is observed along the return trip when $w_\star$ is kept fixed and finite in the round-trip KZ protocols.

However, we stress that the dynamic scaling behavior is nicely observed when keeping $\Theta_\star$ fixed, even along the return trajectory. This may be related to fact that, when keeping $\Theta_\star$ fixed, the time scaling variable $\Theta_\star$ remains finite, therefore the time variable is always rescaled consistently with the time scale of the equilibrium quantum transition, provided by the inverse gap at the transition, i.e. $\Delta \sim L^{-z}$ at the critical point, or $\Delta \sim \lambda^{-z}$ in the thermodynamic limit, where λ is the KZ length scale . As a consequence, the interval of values of $w(t)$ remains limited within a small interval around the transition, which becomes smaller and smaller in the large-size limit, as $|w| \lesssim L^{-y_w}$, and the relative quantum phases behave consistently with the scaling laws.

2.4 Summary

We address these issues within many-body model undergoing quantum transitions, exploiting a unified RG framework, where general dynamic scaling laws are derived in the large-t_s and large-L limits. In particular, we extend the RG framework already developed for standard KZ protocols.

The observation of scaling behavior along the return way turns out to be more problematic, due to the persistence of rapidly oscillating relative phases between

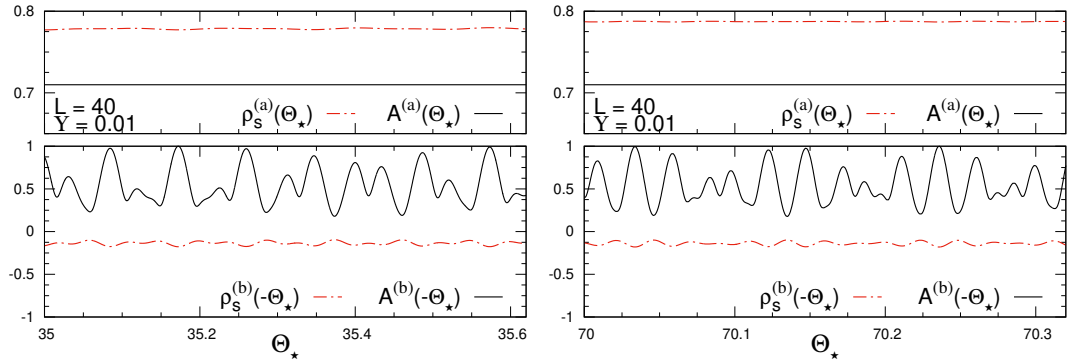

Figure 2.3: Behavior of the subtracted particle density ρ_s and the adiabaticity function A for the Kitaev wire, for fixed $L = 40$, $\Upsilon = 0.01$ versus $\Theta_\star$, close to $\Theta_\star = 70$ (bottom figure) and $\Theta_\star = 35$ (top figure). In each figure, the top plot the values of $\rho_s^{(a)}$ and $A^{(a)}$ at the end of the outward branch, corresponding to $\Theta = \Theta_\star$, while the bottom plot shows the values of $\rho_s^{(b)}$ and $A^{(b)}$ at the end of the return branch, corresponding to $\Theta = -\Theta_\star$. Again, the comparison of the top and bottom figures show that the oscillations tend to become more frequent with increasing $\Theta_\star$.

the relevant quantum states. They make the return way extremely sensitive to the parameters of the protocol, such as the extreme value w_f and the size L of the system. This is essentially related to the quantum nature of the dynamics. Indeed there are some notable similarities with the behavior of quantum two-level models subject to round-trip protocols, analogous the well-known Landau-Zener-Stückelberg problem [62].

Chapter 3

Dissipation

3.1 From local to uniform dissipation: the sunburst model

We consider a lattice model tailored to unveil the crossover regime between the dissipation schemes presented. We investigate a $(1+1)$-dimensional Kitaev ring with local particle-decay dissipators arranged in a *sunburst* geometry [39, 40, 41]. The whole apparatus is sketched in Fig. 3.1. The open quantum system is coupled with the environment by means of $n \equiv L/b$ equally-spaced external baths, which reduce to some extent the translation invariance of the starting model. In particular, we focus on the case of particle-decay jump operators in the Eq.(1.7), i.e., $\hat{L}_x = \hat{c}_x$, where fermionic particles are continuously removed from the site x. With this choice, the Liouville operator $\mathcal{L}$ is quadratic in the fermionic variables $\hat{c}_x$ and $\hat{c}_x^\dagger$, and, in this sense, we say that the open ring we study maintains its integrability. Most of the results discussed in this work should preserve their validity also for particle-pumping dissipation ($\hat{L}_x = c_x^\dagger$), since Eq. (1.7) is still quadratic in the fermionic creation and annihilation operators.

We explore different large-size limits, depending on the number of dissipators taken into account. A thorough study of the Liouvillian gap Δ_λ is the main focus of the first part of this section. In the second part, we examine the real-time evolution of the system, triggered by a *soft quench* of a coupling constant appearing in the defining hamiltonian [1]. Starting the protocol in the proximity of a CQT, we study the out-of-equilibrium dynamic using RG arguments and FSS frameworks [42, 27].

We emphasize the interplay between the unitary and dissipative dynamics and the role played by the gap Δ_λ, extending some of the results already presented in Ref. [64] to our model. To outline our FSS theory, we mainly focus on the scaling properties of the critical correlations and one of the most common entanglement quantifiers, i.e., the entanglement entropy [65].

[1] In a *soft quench* the variation of the quenched parameter is attenuated down to 0 with increasing the lattice size L.

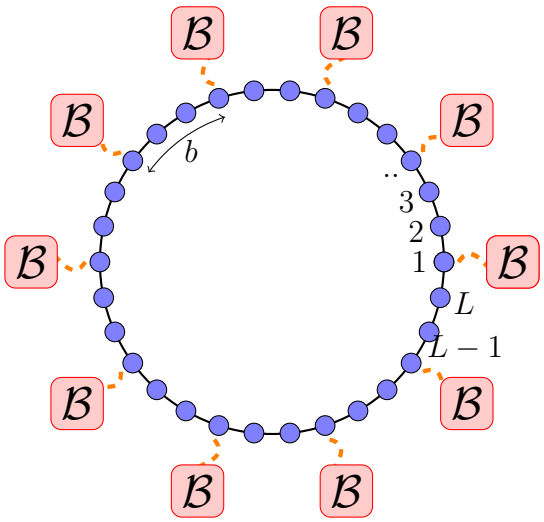

Figure 3.1: Sketch of a Kitaev ring with $L = 30$ qubits coupled with $n = 10$ dissipators in a *sunburst* geometry ($b = 3$ in the figure).

3.1.1 Liouvillian Gap

This section is devoted to discussing the different scaling behaviors observed for the Liouvillian gap Δ_λ defined in the subsection 1.4.2. We will consider two different limits, depending on the number of dissipation sources considered with increasing the lattice size.

Liouvillian gap at fixed b

The value of the Liouvillian gap at fixed b can be computed using two different algorithm. One, useful for small value of b, consists to analyze the system in the Fourier space the Lindblad vectorized Eq. (1.12) whose spectrum gives the gap.

The latter uses the third quantization technique, see details in Ref. [66], particularly convenient for high value of the parameter b [38]. Without loss of generality, we will focus only on small values of b, i.e. up to $b = 7$, but all the results can be extended also in the case of high $b > 7$.

For $b = 3$, the Liouville gap Δ_λ shows a behavior in terms of w in Fig. 3.2. At fixed L, we can easily distinguish two different regimes for the gap, which are separated by a bump in the gap located at $w_*(L)$. We clarify that a non-monotone trend in Δ_λ is not unexpected due to the presence of the *quantum Zeno effect* — the dynamic of a quantum system slows down when it is frequently monitored [67, 68]. Note also that both $w_*(L)$ and $\Delta_\lambda(w_*)$ vanish in the thermodynamic limit, so only the region with $w \geq w_*$ is relevant to determine the typical relaxation time of the system for large enough ring sizes. As shown in Fig. 3.2, for $w < w_*$, the gap is perfectly compatible with a linear dependence of the form

$$\Delta_\lambda(w, b) = \frac{w}{2b}, \quad w < w_*\,. \tag{3.1}$$

We have verified numerically that the above expression holds also for different values of $b \leq 7$ (not shown). This equation has a clear interpretation when we rewrite $\mathbb{D}[\rho]$ in momentum space. Indeed, the full Hilbert space decomposes into

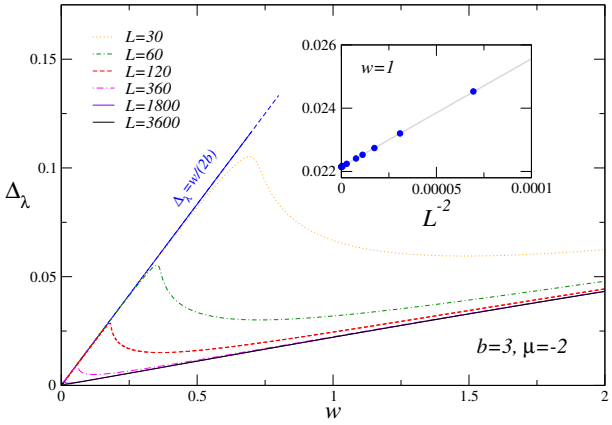

Figure 3.2: Liouvillian gap Δ_λ in terms of the dissipation coupling w for $b = 3$ and fixed $\mu = -2$. For small w and L finite, the gap depends linearly on the dissipation strength as $\Delta_\lambda = w/2b$. With increasing L and finite $w > 0$, the Liouvillian gap approaches a different regime, which still depends linearly on w. In the inset, scaling corrections evaluated at $w = 1$ are perfectly consistent with a L^{-2} decaying. The gray straight line is drawn to guide the eye.

the direct product of $n/2$ distinguished sectors with a dimension 4^b. The effective coupling perceived within each sector is equal to w/b. If we additionally assume that the minimum contribution stemming from a single sector is $1/2$ (which is always the case for $b = 1$), we get Eq. (3.1).

On the other hand, when $w > w_*$, we observe that the gap Δ_λ still depends linearly on the coupling w, but the slope of the asymptotic straight line approached is no longer $1/2b$. We conjecture that for $w > w_*$ and sufficiently large b, the following expression describes the Liouvillian gap

$$\Delta_\lambda(w, b) = A_\mu(b)w\,, \quad A_\mu(b) = \frac{C_\mu}{b^3}\,, \quad w > w_*\,, \tag{3.2}$$

where C_μ is a constant that only depends on the chemical potential μ. Matching arguments with the boundary-dissipation cases surely prompted our guess. Indeed, when $b \propto L$, we expect to recover the leading behavior $\Delta_\lambda \sim L^{-3}$ frequently observed in the literature. Our ansatz is fully supported by the data that we have collected for A_μ in terms of $1/b^3$, as shown in Fig. 3.3 [1]. Indeed, a straight line with a slope of $C_\mu = 0.601(3)$ describes our data for all values of $b \geq 3$ considered ($\chi^2/\text{ndof} = 1.0$).

We also want to mention a scaling regime observed for $L\Delta_\lambda$ in terms of wL when the latter quantity is kept fixed in the large size limit. In Fig. 3.4, we report our data for $b = 2, \mu = -3$ and $b = 4, \mu = -1$.

Liouvillian gap at fixed n

Now we start to study the behavior when we keep $n = L/b$ fixed. Since the number of the external baths scales with the system size L, we will apply the third quantization technique, cited above.

[1] Systematic error bars reported in the figure have been estimated from the comparison of $A_\mu(b)$ for different lattice sizes $L \geq L_{\min}$ and coupling ranges $w \geq w_{\min}$.

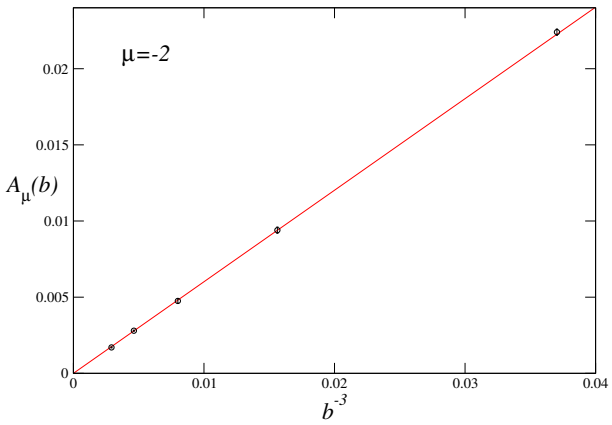

Figure 3.3: Liouvillian rate coefficient $A_\mu(b)$ versus b^{-3} with constant $\mu = -2$. For $b \geq 3$, we observe that $A_\mu(b)$ is compatible with a power-law dependence of the form $A_\mu(b) = C_\mu/b^3$, where $C_\mu = 0.601(3)$ ($\chi^2/\text{ndof} = 1.0$).

The Fig. 3.5 shows that the gap scales as $\Delta_\lambda \sim L^{-3}$ at fixed w in the regime $w > w_*$ ($w_\star$ is the maximum point). This scaling is correlated also to the Eq.(3.2) and simple matching arguments.

Referring to Fig. 3.5, when $w < w_*$ the gap does not show a uniform limit for $w \to 0^+$ as the maximum of $L^3\Delta_\lambda$ grows without bounds with increasing L. We shed some light on this peculiar trend in Fig. 3.6, considering the structure of the gap in the proximity of $w = 0$ at fixed $n = 10$ and $\mu = -1$. In fact, the plot supports the existence of a scaling regime for $L^2\Delta_\lambda$ when w is properly rescaled as $w \sim 1/L$. Scaling corrections are also compatible with a decaying L^{-2}, as shown in the corresponding inset. We stress again that numerical results for different values of μ do not exhibit remarkable differences. We conclude that the different scaling regimes shown by the Liouvillian gap do not depend either on μ or the quantum phase related to the Kitaev model.

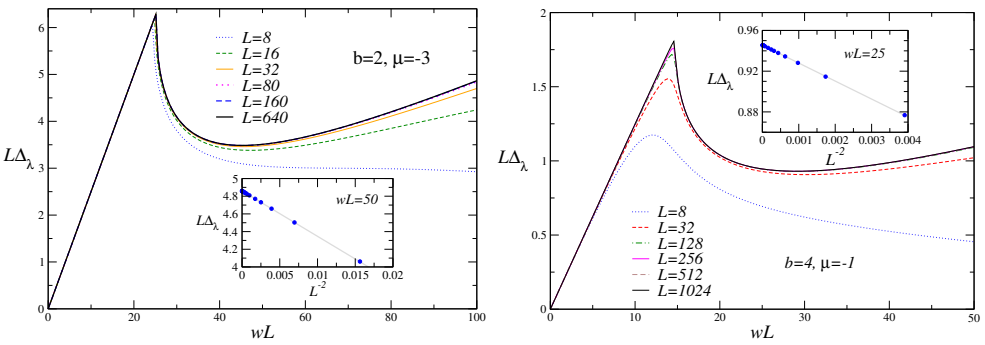

Figure 3.4: Scaling of $L\Delta_\lambda$ versus wL for different values of b and μ. On the top panel, we show results for $b = 2$ and $\mu = -3$, while on the bottom panel, we fix $b = 4$ and $\mu = -1$. The figures show an excellent data collapse in agreement with L^{-2} scaling corrections. The straight lines in the insets are drawn to guide the eye.

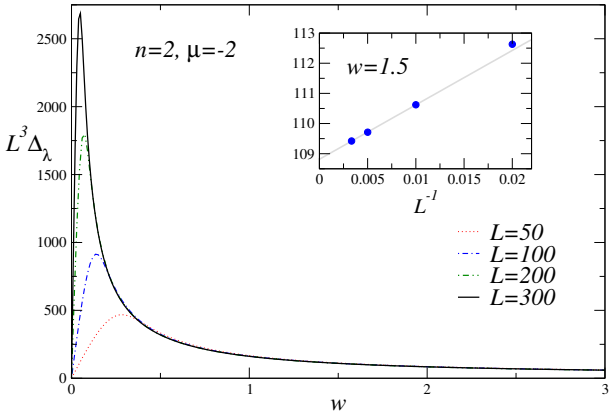

Figure 3.5: Plot of the rescaled gap $L^3\Delta_\lambda$ in terms of w for fixed $n = 2$ and $\mu = -2$. At fixed w, the gap shows a nice data collapse within L^{-1} scaling corrections, as provided by the inset for the case $w = 1.5$. The straight line is drawn to guide the eye.

3.1.2 Dynamic FSS Framework

In this section, we study the time evolution of the Kitaev ring in the proximity of a CQT. To this end, we exploit a dynamic FSS framework and use RG arguments to describe the evolution of the critical correlations. Concerning the algorithms adopted, we speed up our simulations by moving to the momentum basis every time we maintain b fixed. On the other hand, when n is fixed, we just monitor the evolution of the two-point correlation functions by solving a closed system of differential equations. To evolve the density matrix ρ in time, we use standard 4^{th}-order Runge-Kutta techniques with typical integration time steps of $\Delta t = 0.01$.

The quench protocol and the monitored observables

We now present the quench protocol considered to study the time evolution of the open quantum system under scrutiny at CQTs. We prepare the system in the ground state $|\Omega\rangle$ of Eq. (1.4). The starting chemical potential μ_i is always close to

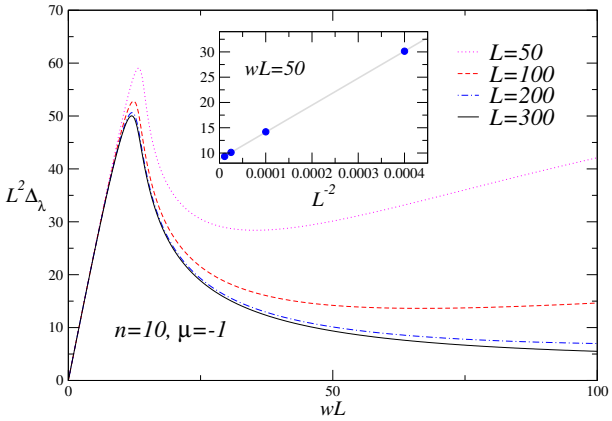

Figure 3.6: The figure shows the Liouvillian gap $L^2\Delta_\lambda$ versus w at fixed $n = 10$ for $\mu = -1$. In the inset, scaling corrections at $wL = 50$ are consistent with a decay L^{-2}. The straight line is drawn to guide the eye.

the critical value μ_c, meaning that $|\mu_i - \mu_c| \to 0$ for $L \to \infty$. At a reference time $t = 0$, the ring is driven out-of-equilibrium by suddenly coupling the system with the surrounding environment and eventually quenching the chemical potential to a different value $\mu_i \to \mu_f$. In such a case, the final μ_f should always be sufficiently close to the critical point.

We monitor the time evolution of the Kitaev ring by considering two distinguished two-point correlation functions $C(x, y, t)$ and $P(x, y, t)$, defined as

$$C(x, y, t) \equiv \mathrm{Tr}[\rho(t)(\hat{c}_x^\dagger \hat{c}_y + \hat{c}_y^\dagger \hat{c}_x)] \,, \tag{3.3}$$

$$P(x, y, t) \equiv \mathrm{Tr}[\rho(t)(\hat{c}_x^\dagger \hat{c}_y^\dagger + \hat{c}_y \hat{c}_x)] \,. \tag{3.4}$$

3.1.3 Out-of-equilibrium FSS frameworks at CQTs with b fixed

To describe the time evolution of the system under study at CQTs, we employ RG arguments and a dynamic FSS framework [42, 27]. The interplay between the unitary and dissipative dynamics of a Kitaev ring subject to complete bulk dissipation ($b = 1$) has already been addressed in Ref. [64]. The results presented in this section extend the FSS reported in that work to all the cases with fixed $b > 1$, and provide a complementing discussion on the role of Δ_λ in such a regime. Let us first review the main ideas leading to the FSS theory that we are going to discuss.

When we consider the time evolution of an open quantum system after a quench, analogous equations are more involved given the presence of a larger number of scaling quantities and relevant perturbations. First of all, we need to introduce a pre- and a post-quench scaling field $M_{i/f} = (\mu_{i/f} - \mu_c)L^{y_\mu}$ for μ. In the second place, the time variable t requires a scaling field as well. The most natural guess, which also turns out to be the correct one in most cases, is to rescale t with L on the basis of the dynamic critical exponent z. We then introduce the quantity Θ defined as

$$\Theta = tL^{-z} \,, \quad z = 1 \,, \tag{3.5}$$

which is maintained constant in the FSS limit. Since the number of particle-decay jump operators increases as L, we also need to soften the coupling w to observe an interplay between the critical and dissipative modes. We note that the parameter w plays the role of a decay rate, namely, it is an inverse relaxation time [64, 26]. In our work hypothesis, we then suppose that w should be rescaled with L^{-z} to observe universal FSS relations. We introduce the scaling field γ_b as

$$\gamma_b = \frac{wL^z}{b} \,, \quad z = 1. \tag{3.6}$$

Naturally, the prefactor b^{-1} appearing in γ_b is just a matter of convention if one restricts the analysis to just one value of b. However, the comparison between different values of b in the FSS limit may add new valuable insights to our analyses. To compare the dissipative processes of different rings on the same footing, we assume that the effective coupling strength is w/b. This choice is the most natural one considering the Kitaev ring in momentum space.

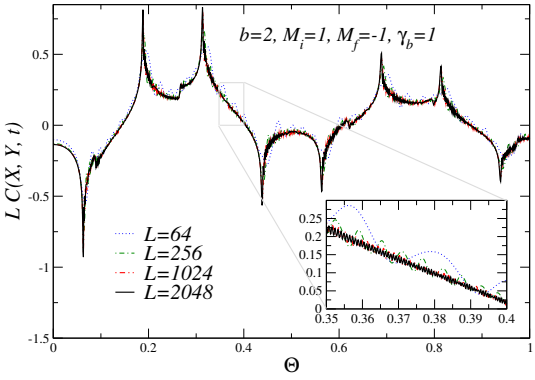

Figure 3.7: Scaling of the two-point function $LC(X,Y)$ in terms of the scaling variable Θ for fixed $b=2$, $M_i=1$ and $\gamma_b=1$. We consider $(Y-X)/L=1/4$ and fix $x=1$, using translation invariance. In the inset, we show a zoom of the region $\Theta\in[0.35,0.4]$. Our data clearly support the FSS laws exhibited in Eq.(3.7).

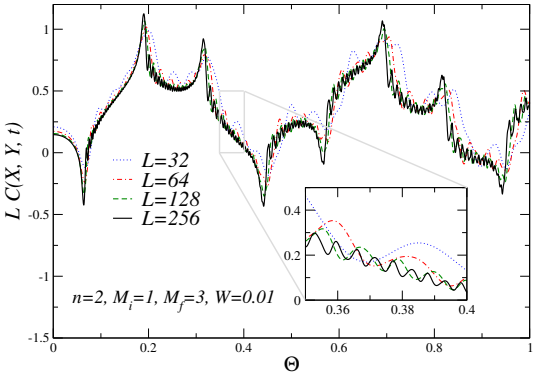

Figure 3.8: Scaling of the rescaled two-point correlation function $LC(X,Y)$ in terms of Θ for fixed of $n=2, M_i=1, M_f=3$, and $W=0.01$. We consider $Y-X=L/4$, exploiting translation invariance, and fix the first site to $x=1$ in conjunction with a dissipator. We zoom in on the domain $\Theta\in[0.35,0.4]$ to emphasize the convergence of different curves with increasing lattice size L.

The universal scaling relations satisfied by the two-point functions C and P in Eq. (3.4) follows

$$C(x,y,t)\approx L^{-2y_c}\mathcal{C}(M_i,M_f,\{X_i\},\Theta,\gamma_b) \tag{3.7}$$
$$P(x,y,t)\approx L^{-2y_c}\mathcal{P}(M_i,M_f,\{X_i\},\Theta,\gamma_b)\,, \tag{3.8}$$

where $y_c=1/2$ is the scaling dimension of both $\hat{c}$ and $\hat{c}^\dagger$. In Fig. 3.7 we show the scaling of $LC(X,Y,t)$ in terms of the scaling quantity Θ for $b=2$, $M_i=1$, $M_f=-1$, and $\gamma_b=1$. The panel definitely supports the FSS laws exhibited in Eq. (3.7). In the inset, we show that the amplitude of the oscillations reduces at fixed Θ and increasing L, roughly as $\sim L^{-1/2}$. We have checked that Eq. (3.8) holds also for the scaling of the RG invariant quantity $LP(X,Y,t)$ (not shown).

3.1.4 Out-of-equilibrium FSS framework at CQTs with n fixed

In this section, we derive a dynamic FSS framework at CQTs to study the time evolution of Eq. (1.7) when the number of the dissipators n is fixed. Most of the scaling relations of the last section are still valid at fixed n with straightforward generalizations. In particular, we just replace the coupling w in our relations, which now represents a decay rate per unit space since $b \sim L$. As a working hypothesis, we expect the scaling field W, defined as

$$W = wL^{z-1}\,, \quad z = 1\,, \tag{3.9}$$

to be a reasonable scaling quantity in the FSS limit. For instance, the critical correlations satisfy scaling relations similar to the ones reported in Eq. (3.7)

$$C(x,y,t) \approx L^{-2y_c}\mathcal{C}(M_i, M_f, \{X_i\}, \Theta, W) \tag{3.10}$$
$$P(x,y,t) \approx L^{-2y_c}\mathcal{P}(M_i, M_f, \{X_i\}, \Theta, W)\,. \tag{3.11}$$

We verify our hypotheses in Fig. 3.8, showing the scaling curve for $LC(X,Y,t)$ versus the scaling variable Θ with constant $n = 2, M_i = 1, M_f = 3, W = 0.01$. We obtain a nice data collapse considering lattice sizes up to $L = 256$. The oscillation amplitudes shrink with increasing L, converging to a universal asymptotic curve $\mathcal{C}$. The validity of Eq. (3.11) has been checked also by inspecting the time evolution of $LP(X,Y,t)$ (not shown).

3.2 Summary

When we keep b fixed, the gap Δ_λ is always finite and depends linearly on the dissipation strength w. Nonetheless, two different regimes emerge for systems of finite size. In the small w region, the gap is given by $\Delta_\lambda = w/(2b)$, whereas, at large w and sufficiently large b, it behaves as $\Delta_\lambda = wC_\mu/b^3$. The last equation always controls the gap in the large-size limit and is our starting point to deduce the scaling of such a quantity when $b \propto L$. It is worth mentioning that we also put forward a scaling regime for $L\Delta_\lambda$ as a function of wL, which ties together the two different regimes outlined in a smooth manner. On the other hand, when we keep the number of dissipators n fixed, the gap vanishes as $\sim L^{-3}$ at large L. Addressing the structure of the gap at small w, we find a scaling regime for $L^2\Delta_\lambda$ in terms of wL, which is closely related to the presence of a non-uniform convergence of $L^3\Delta_\lambda$ in the limit $w \to 0^+$.

We develop a dynamic FSS regime at CQTs to describe the time evolution of the Kitaev model under investigation. At fixed b, our results extend the FSS theory of Ref. [64] to the cases with $b > 1$. As a working hypothesis, we suppose that the scaling variable associated with the relevant coupling w is $\gamma_b = wL^z/b$. Our numerical results for the two-point correlation functions fully support this ansatz. When the number of dissipators n is fixed, the FSS theory outlined at fixed b generalizes straightforwardly after replacing γ_b with $W = wL^{z-1}$.

Conclusions

We have studied the out-of-equilibrium behavior of many-body systems when their time-dependent Hamiltonian parameters slowly cross phase transition points. In particular, we present an exploratory study of out-of-equilibrium behaviors arising from round-trip protocols across quantum phase transitions.

As paradigmatic model we choose the Kitaev model which is mapped in the transverse quantum Ising model through a JW transformation. Indeed, all the results are valid also in the case of the longitudinal Ising model [62] where the longitudinal magnetic field drives the round-trip KZ protocol. Note that, in the case of one-dimensional quantum Ising model, the slow variation of the longitudinal field across the CQT point brings the system from a gapped condition to another gapped condition, i.e. move the system from disorder to disorder through a CQT. Therefore, this is not the standard situation of the KZ problem related to the defect production going from the disorder to the order phases.

The emerging dynamic scaling scenario put forward for round-trip KZ protocols across critical points is expected to hold for generic classical and quantum transitions separating phases with short-range correlations, in any spatial dimension. Further investigations are called for round-trip protocols between disordered and ordered phases, when the ordered phase has gapless excitations. Round-trip KZ protocols in these systems may show further interesting features.

Indeed, we believe that also the chaotic-like return way calls for further investigation. Even in the simple two-level quantum model some features of the behavior along the return way turn out not to be smooth [62, 69]. Indeed, they develop ample oscillations with larger and larger frequencies when increasing the interval of the round-trip variation of the parameters.

In the second part, we have considered a Kitaev ring coupled with the environment via n particle-decay dissipators arranged in a sunburst geometry.

We analyze the interplay between the Liouvillian gap Δ_λ and the gap related to the Kitaev ring Δ in the FSS limit. In particular, we take into account the short- and long-time regimes, focusing on how they join together in the FSS limit. When b is fixed, we observe that the link between the two regimes is smooth, whereas, at fixed n, the two regions can be easily distinguished given the presence of different power-law scalings for the gaps Δ and Δ_λ.

As future outlooks, we mention that the results of the round-trip KZ protocol and of the Liouvillian gap analysis can be extended in several directions. First of all, our studies can be generalized by considering thermal baths in the Lindblad formalism [70]. Alternatively, it would be interesting to understand how the different large-size limits considered in this paper affect the Liouville gap and the

FSS regime of open quantum models in higher dimensions. Despite the numerous challenges given by such a quest, we must say that this setting certainly offers attractive questions and new paradigms to be addressed. To name a few, we mention that the NESS, in more than one spatial dimension, may undergo a continuous phase transition, similar to a finite-temperature quantum system at equilibrium. For this reason, the evolutions of open quantum models in the short- and long-time regimes can be associated with different RG fixed points, entailing a more intriguing scenario in the FSS limit.

We conclude by mentioning that the results for the round-trip KZ protocol are also extended for first order transitions [69] in which we can approximate the many-body system as a 2-level model within the scaling regime.

References

[1] Anatoli Polkovnikov et al., "Colloquium: Nonequilibrium dynamics of closed interacting quantum systems", Rev. Mod. Phys. **83**, 863–883 (2011).

[2] I. M. Georgescu, S. Ashhab, and Franco Nori, "Quantum simulation", Rev. Mod. Phys. **86**, 153–185 (2014).

[3] Marton Kormos et al., "Real-time confinement following a quantum quench to a non-integrable model", Nature Physics **13**, 246–249 (2017).

[4] Alessio Lerose et al., "Quasilocalized dynamics from confinement of quantum excitations", Physical Review B **102**, 041118 (2020).

[5] Riccardo Javier Valencia Tortora, Pasquale Calabrese, and Mario Collura, "Relaxation of the order-parameter statistics and dynamical confinement", Europhysics Letters **132**, 50001 (2020).

[6] Gianluca Lagnese et al., "Quenches and confinement in a heisenberg–ising spin ladder", Journal of Physics A: Mathematical and Theoretical **55**, 124003 (2022).

[7] Stefano Scopa, Pasquale Calabrese, and Alvise Bastianello, "Entanglement dynamics in confining spin chains", Physical Review B **105**, 125413 (2022).

[8] Olalla A Castro-Alvaredo et al., "Entanglement oscillations near a quantum critical point", Physical Review Letters **124**, 230601 (2020).

[9] Joseph Vovrosh and Johannes Knolle, "Confinement and entanglement dynamics on a digital quantum computer", Scientific reports **11**, 11577 (2021).

[10] Marco Rigobello et al., "Entanglement generation in (1+ 1) D QED scattering processes", Physical Review D **104**, 114501 (2021).

[11] Stefan Birnkammer, Alvise Bastianello, and Michael Knap, "Prethermalization in one-dimensional quantum many-body systems with confinement", Nature Communications **13**, 7663 (2022).

[12] Andrew JA James, Robert M Konik, and Neil J Robinson, "Nonthermal states arising from confinement in one and two dimensions", Physical review letters **122**, 130603 (2019).

[13] Neil J Robinson, Andrew JA James, and Robert M Konik, "Signatures of rare states and thermalization in a theory with confinement", Physical Review B **99**, 195108 (2019).

[14] Titas Chanda et al., "Confinement and lack of thermalization after quenches in the bosonic Schwinger model", Physical Review Letters **124**, 180602 (2020).

[15] Leandro Aolita, Fernando de Melo, and Luiz Davidovich, "Open-system dynamics of entanglement:a key issues review", Reports on Progress in Physics **78**, 042001 (2015).

[16] Thomas WB Kibble, "Topology of cosmic domains and strings", Journal of Physics A: Mathematical and General **9**, 1387 (1976).

[17] Tom WB Kibble, "Some implications of a cosmological phase transition", Physics Reports **67**, 183–199 (1980).

[18] Wojciech H Zurek, "Cosmological experiments in superfluid helium?", Nature **317**, 505–508 (1985).

[19] Wojciech H Zurek, "Cosmological experiments in condensed matter systems", Physics Reports **276**, 177–221 (1996).

[20] Kurt Binder, "Theory of first-order phase transitions", Reports on progress in physics **50**, 783 (1987).

[21] Jin-Ming Cui et al., "Experimentally testing quantum critical dynamics beyond the Kibble–Zurek mechanism", Communications Physics **3**, 44 (2020).

[22] Alan J Bray, "Theory of phase-ordering kinetics", Advances in Physics **51**, 481–587 (2002).

[23] Chad N Weiler et al., "Spontaneous vortices in the formation of Bose–Einstein condensates", Nature **455**, 948–951 (2008).

[24] Jacek Dziarmaga, "Dynamics of a quantum phase transition and relaxation to a steady state", Advances in Physics **59**, 1063–1189 (2010).

[25] S Ulm et al., "Observation of the Kibble–Zurek scaling law for defect formation in ion crystals", Nature communications **4**, 2290 (2013).

[26] H. P. Breuer and F. Petruccione, "The theory of open quantum systems", Oxford University Press, 2002.

[27] Davide Rossini and Ettore Vicari, "Coherent and dissipative dynamics at quantum phase transitions", Physics Reports **936**, 1–110 (2021).

[28] L M Sieberer, M Buchhold, and S Diehl, "Keldysh field theory for driven open quantum systems", Reports on Progress in Physics **79**, 096001 (2016).

[29] Davide Nigro, "On the uniqueness of the steady-state solution of the Lindblad–Gorini–Kossakowski–Sudarshan equation", Journal of Statistical Mechanics: Theory and Experiment **2019**, 043202 (2019).

[30] S. G. Schirmer and Xiaoting Wang, "Stabilizing open quantum systems by Markovian reservoir engineering", Phys. Rev. A **81**, 062306 (2010).

[31] Fernando Pastawski, Lucas Clemente, and Juan Ignacio Cirac, "Quantum memories based on engineered dissipation", Phys. Rev. A **83**, 012304 (2011).

[32] Marko Znidaric, "Relaxation times of dissipative many-body quantum systems", Phys. Rev. E **92**, 042143 (2015).

[33] Dong Yuan et al., "Solving the Liouvillian Gap with Artificial Neural Networks", Phys. Rev. Lett. **126**, 160401 (2021).

[34] Naoyuki Shibata and Hosho Katsura, "Dissipative spin chain as a non-Hermitian Kitaev ladder", Phys. Rev. B **99**, 174303 (2019).

[35] Naoyuki Shibata and Hosho Katsura, "Quantum Ising chain with boundary dephasing", PTEP **2020**, 12 (2020).

[36] Francesco Tarantelli and Ettore Vicari, "Quantum critical systems with dissipative boundaries", Phys. Rev. B **104**, 075140 (2021).

[37] Marko Žnidarič, "Transport in a one-dimensional isotropic Heisenberg model at high temperature", Journal of Statistical Mechanics: Theory and Experiment **2011**, P12008 (2011).

[38] Alessio Franchi and Francesco Tarantelli, "Liouvillian gap and out-of-equilibrium dynamics of a sunburst Kitaev ring: from local to uniform dissipation", arXiv:2305.04207 , (2023).

[39] Alessio Franchi, Davide Rossini, and Ettore Vicari, "Quantum many-body spin rings coupled to ancillary spins: The sunburst quantum Ising model", Phys. Rev. E **105**, 054111 (2022).

[40] Alessio Franchi, Davide Rossini, and Ettore Vicari, "Decoherence and energy flow in the sunburst quantum Ising model", Journal of Statistical Mechanics **2022**, 083103 (2022).

[41] Akash Mitra and Shashi C. L. Srivastava, "Quantum sunburst model under interaction quench: entanglement and role of initial state coherence", arXiv:2212.12276 , (2022).

[42] John Cardy, "Scaling and Renormalization in Statistical Physics", Cambridge Lecture Notes in Physics, Cambridge University Press, 1996.

[43] Subir Sachdev, "Quantum phase transitions", 4, Cambridge University Press, 1999.

[44] Andrea Pelissetto and Ettore Vicari, "Critical phenomena and renormalization-group theory", ISSN: 0370-1573, Physics Reports **368**, 549–727 (2002).

[45] Massimo Campostrini, Andrea Pelissetto, and Ettore Vicari, "Finite-size scaling at quantum transitions", Phys. Rev. B **89**, 094516 (2014).

[46] Andrea Pelissetto and Ettore Vicari, "Scaling behaviors at quantum and classical first-order transitions", arXiv preprint arXiv:2302.08238 , (2023).

[47] Anushya Chandran et al., "Kibble-Zurek problem: Universality and the scaling limit", Physical Review B **86**, 064304 (2012).

[48] Andrea Pelissetto, Davide Rossini, and Ettore Vicari, "Scaling properties of the dynamics at first-order quantum transitions when boundary conditions favor one of the two phases", Physical Review E **102**, 012143 (2020).

[49] Haralambos Panagopoulos, Andrea Pelissetto, and Ettore Vicari, "Dynamic scaling behavior at thermal first-order transitions in systems with disordered boundary conditions", Physical Review D **98**, 074507 (2018).

[50] Massimo Campostrini, Andrea Pelissetto, and Ettore Vicari, "Quantum Ising chains with boundary fields", Journal of Statistical Mechanics: Theory and Experiment **2015**, P11015 (2015).

[51] Andrea Pelissetto, Davide Rossini, and Ettore Vicari, "Finite-size scaling at first-order quantum transitions when boundary conditions favor one of the two phases", Physical Review E **98**, 032124 (2018).

[52] Davide Rossini and Ettore Vicari, "Ground-state fidelity at first-order quantum transitions", Physical Review E **98**, 062137 (2018).

[53] GG Cabrera and R Jullien, "Role of boundary conditions in the finite-size Ising model", Physical Review B **35**, 7062 (1987).

[54] Massimo Campostrini et al., "Finite-size scaling at first-order quantum transitions", Physical review letters **113**, 070402 (2014).

[55] A Yu Kitaev, "Unpaired Majorana fermions in quantum wires", Physics-Uspekhi **44**, 131 (2001).

[56] Pierre Pfeuty, "The one-dimensional Ising model with a transverse field", ISSN: 0003-4916, Annals of Physics **57**, 79–90 (1970).

[57] Wojciech H Zurek, Uwe Dorner, and Peter Zoller, "Dynamics of a quantum phase transition", Physical review letters **95**, 105701 (2005).

[58] Davide Rossini and Ettore Vicari, "Coherent and dissipative dynamics at quantum phase transitions", Physics Reports **936**, 1–110 (2021).

[59] Francesco Tarantelli and Ettore Vicari, "Out-of-equilibrium quantum dynamics of fermionic gases in the presence of localized particle loss", Phys. Rev. A **105**, 042214 (2022).

[60] Michael Zwolak and Guifré Vidal, "Mixed-State Dynamics in One-Dimensional Quantum Lattice Systems: A Time-Dependent Superoperator Renormalization Algorithm", Phys. Rev. Lett. **93**, 207205 (2004).

[61] Davide Rossini and Ettore Vicari, "Dynamic Kibble-Zurek scaling framework for open dissipative many-body systems crossing quantum transitions", Physical Review Research **2**, 023211 (2020).

[62] Francesco Tarantelli and Ettore Vicari, "Out-of-equilibrium dynamics arising from slow round-trip variations of Hamiltonian parameters across quantum and classical critical points", Physical Review B **105**, 235124 (2022).

[63] J. P. Blaizot and G. Ripka, "Quantum Theory of Finite Systems", Cambridge, Massachusetts: The MIT Press, 1986.

[64] Davide Nigro, Davide Rossini, and Ettore Vicari, "Competing coherent and dissipative dynamics close to quantum criticality", Phys. Rev. A **100**, 052108 (2019).

[65] Yi-Neng Zhou, Liang Mao, and Hui Zhai, "Rényi entropy dynamics and Lindblad spectrum for open quantum systems", Phys. Rev. Research **3**, 043060 (2021).

[66] Tomaž Prosen, "Third quantization: a general method to solve master equations for quadratic open Fermi systems", New Journal of Physics **10**, 043026 (2008).

[67] B. Misra and E. C. G. Sudarshan, "The Zeno's paradox in quantum theory", Journal of Mathematical Physics **18**, 756–763 (1977).

[68] Taiki Haga et al., "Quasiparticles of Decoherence Processes in Open Quantum Many-Body Systems: Incoherentons", arXiv:2211.14991 , (2022).

[69] Francesco Tarantelli and Stefano Scopa, "Out-of-equilibrium scaling behavior arising during round-trip protocols across a quantum first-order transition", arXiv:2305.12993 , (2023).

[70] Francesco Tarantelli and Ettore Vicari, "Thermal bath effects in quantum quenches within quantum critical regimes", Phys. Rev. B **108**, 035128 (2023).